Journal of Engineering Science and Technology
Vol. 16, No. 6 (2021) 4833 - 4852

FINITE ELEMENT DYNAMIC ANALYSIS OF THIN SHELLS SUBJECTED TO ARBITRARY LOADING

AHMED ABDULLAH MANSOR*,
MARAWAN M. HAMID, NARJIS SABIH ABBAS

College of Engineering, University of Diyala, Iraq
*Corresponding Author: aamansor@engineering.uodiyala.edu.iq

Abstract

A mixture of the compensations of the reduced of Fourier series extension in the third dimensions (semi-analytical procedure) and two-dimensional finite element procedure are adapted to execute dynamic analysis of rotational axisymmetric shells due to random loading types. This procedure is depending for decreases the computer charge and expand the computational competence also time as well as exact results can be obtained. A three-nodded quadratic isoperimetric axisymmetric shell element is selected to mobilize the shell buildings. The computer program called (DAASNL) is established for dynamic and static analysis of arbitrary revolution loaded shells. This program is easy to use with less time for different civil engineering problems with different loading cases. FORTRAN language used for writing this program. Finite element formulation equations of motion are presented and discussed as well as outlined of method solution. The geometry effects, thickness, shallowness, configuration of mesh, boundary conditions and Gaussian integration were presented. Orderly for validate the pertinency for anticipated element depend in the current paper for the dynamic analysis also to explain the improved capability of program in the analysis of axisymmetric bodies under dynamic loading and general static, as well as some cases were presented. The presented cases had been measured in available books and papers so as to comparison of found solution with other analytical solutions for the purpose of verification. Adequate and competent results are found. The study results show that using three node degenerated element conjugate with the semi-analytical standard method is exact dependable also delivers exact solution related to dynamic analysis and astatic even for state of thin shells. For thin shell, an enhancement was appearing in the solution accuracy may accomplished by depending reduced integration method.

Keywords: Axisymmetric shells, Blast loading, Fourier series, Non-symmetric loads, Shells of revolutions, Solid shell element.

1. Introduction

The shell structure may define as a solid range placed between curved surfaces - two closely spaced [1]. Generally, a geometrically of shell is a defined by its the shape of mid surface and thickness. A behaviour of shell is ruled by the behaviour of it surface of central. Shell constructions proposal of greatest effective practise for constructional material for various applications. Occasionally it be some problematic for construct compared with further shapes but if restraint may overwhelm, it is providing an accepted as a best choice for various applications. There are commonly used in, domes, space shell roofs, rockets, aircraft, chimneys, cooling tower and nuclear containment vessels, and so on. It is acceptance in construction because of the resultant low-cost as well as to the accessibility of enormous variation of shapes with more flexibility in architectural. And it may effectively employ for minimal maintenance demands, descriptions of elegance, and functional usage.

Rendering to "thinness ratio", that is refer to a ratio for shell thickness to a curvature radius for a consideration point, shells may be classified as thin or thick. Usually, when the ratio be more than (1/10), so a shell is considered a thick as well as when the ratio be among (1/10 till 1/50), a shell be considered a thin and if a ratio smaller than (1/50), a shell be considered thinner when it be used for an effective carrying load members [1]. The classification of shell as thin or thick should be dependent on real behaviour of the separate shells due to the assumed scheme of carried loads. The ratio of carried load for amount of the material consumed for the situation of the shell is considered very high [2, 3]. That is be considered a very important issue thus far as the efficiency of shell structure is worried. An applying load that spread over the structure of shell due to acting of bending (transverse action) with adding action membrane (in-plane action). For flat plate beneath same load situations grows just moments and transverse forces. The revolution of surface is created through a rotation of the curved plane around of axis in it is plane [4]. The connection of plane that it is contains an axis of a revolution with mid surface is called the "meridian". Slightly horizontal cross section of a revolution for surface is a circle by it is centre placing on a revolution axis, for circles that called as "parallel circles" [1, 5], see Fig. 1.

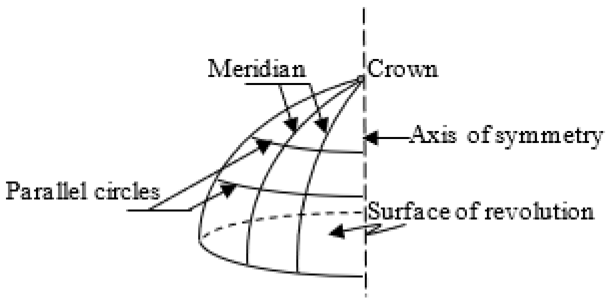

Fig. 1. Shell of revolution [1].

The consideration of several researchers had been concerned by the issues of modelling and empathetic the consequence of shell vibrations due to the blast loads. A limited traditional text has been available in mentioned field: a investigate about a uniform radial instinct for elastic also plastic material response that had been reported in [4]. Amongst of other notifications conclusions, the researcher originates that for under impulsive loads, the modes of buckling take a higher number for circumferential waves, so those static counterparts. So as to get time reliant on pressure flows on a cantilever small scale cylindrical shells shape, the team of France academics achieved experimental research on cylindrical shells with scale factor of 1:48 [5-7]. Knowing the scale factor defined as the ratio of every two corresponding lengths for the two same geometric figures or the proportionality coefficient or the constant proportionality. The objectives of such program testing were to find a probabilistic analysis for threshold values producing a various level of damage. Analytical research depend on Donnell's approximation had been achieved by depending on the static response to be established concert limits depend for plasticity.

Duong et al. [8, 9] investigated a nonlinear dynamic analysis of functionally graded material (FGM) shell structures by depending on a higher order for element solid shell. It was considered an element, the quadratic distribution for shear stress with a thickness. In an FGM, the building be prepared from the combination of metal also ceramic, or the mixture of remained ceramics or remained metals that which suitable to attain the anticipated objective. Properties of materials of shell structure are diverse continuously in a direction of thickness due to all four-limitation power-law distribution on according of a constituent's volume fractions. Accuracy and performance of a current solid-shell (higher order) element are established by comparison the results from the literature and the numerical results found from analyses of finite element.

Ameijeiras and Godoy (2016) [10] presented an analytical result to expect a non-linear forced vibration for flexible thin-walled cylindrical shells due to unexpectedly load. For mentioned model, a kinematic nonlinear relation was depended by Donnell's easy shell theory. The result be achieved for example a sequence's summation for relationships to trigonometric functions for the circumferential also axial directions, although a degrees of freedom hinge on a time. The blast effect be expected to signify effect under explosions on a shell as pressures time dependent by the specified circumferential spreading (a cosine square spreading according to the dominant angle). The obtained results for this model were validated through comparison with the nonlinear finite element model according to a similar condition of load. The effect of a level of load as well as a geometry of shell on a fleeting response is examined by mean of analytical research. Good correctness is initiate for the results of the series shells that were demonstrative in horizontal, oil storage tanks for industry of oil [11].

An axisymmetric structures analysis due to non-symmetric loading lays into a group of semi-analytic procedures. The group of problems are considered by a three-dimensional structure in that material properties as well as geometry are independent for one co-ordinate direction then the applied load might be dependent on the co-ordinate [12]. This technique includes stating the behaviour of the all-pertinent scope variables and load in the co-ordinate due to a Fourier series, therefore minimizing an analysis for uncoupled two-dimensional series analysis.

The topic aim of this study to be developed an effective theoretical method to analysis of axisymmetric shell as well as dome structures for current improved understanding for their behaviour due to the dynamic load depending on a semi-analytical finite element method. The implicit time integration scheme and isoperimetric finite discretization has been used for the reason that these techniques are verified to be greatest effective for extensive series of problems. An elementary principle for isoperimetric elements is which an interpolation functions (shape functions) for displacements are used for representing a geometry for an element. The analysis of axisymmetric structures under non-symmetric loading is of three-dimensional problems in that material properties and geometry are not dependent in one coordinate direction however the applied load can be used on mentioned coordinate as mentioned previously, so Fourier series were used in the present work to reduce the analysis to the series for uncoupled two-dimensional analysis

FORTRAN programming language was used in the present work because it is one for a first (if not a first) high level languages developed of computers. FORTRAN was initially developed practically exclusively of performing numeric computations. This language is more suited to non-numeric operations such as searching databases for information. Also, it is easy to use with less time for different civil engineering problems.

2. Description of Element

The disintegrated quadratic isoperimetric axisymmetric shell element founded on translational displacement interpolation and independent rotational has been adopted here. The element behaviour is based clearly on two basic assumptions: Firstly, ordinary for a mid-surface of shell before deformation that expected for keep on straight but not necessarily normal to it afterward deformation. Secondly, a stress perpendicular to a mid-surface is presumed to be insignificant regardless of loading for their small values.

The element has three nodes through five freedom degrees for each node, three for translational for axial, radial and circumferential directions (u, v, w) and remains are rotational that signify a rotation for a normal at node (α, β). Every node in this element be considered as the nodal circle Fig. 2.

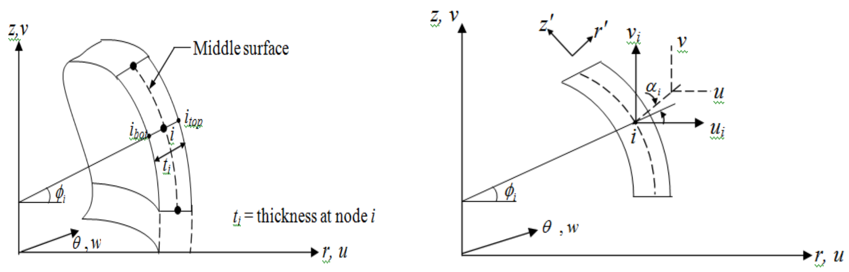

(a) Global cylindrical coordinate system. **(b) Local coordinate system.**

Fig. 2. Degenerated isoperimetric Shell element [13].

Noting that for Fig. 2, $r,\ z,\ \theta r,\ z,\ \theta$ is the system of coordinate Global cylindrical, $r^{'},\ z^{'}r',\ z'$ are the Local coordinate system, $u_i,\ v_i,\ w_i u_i,\ v_i,\ w_i$ are the Transformation freedom degrees, $\alpha_i,\ \beta_i$ are Rotational freedom degrees, ϕ is the meridian direction angle and θ is the circumferential direction angle.

The shape functions for the geometry of shell element along the meridian and the displacement functions are both assumed to be of quadratic form. The variations of both element dependent functions are assumed to vary linearly across the shell thickness. It may be considered which every point in a shell element may description depend on a pair of points in a bottom and a top face for element (i_{top} and i_{bot}) as could be seen in Fig. 2. Each point was with a given cylindrical coordinate. The relation between a global coordinate for each point for shell also a curvilinear coordinate may be writing as mentioned a form in Eq. (1) [13, 14]:

$$\begin{Bmatrix} r \\ z \end{Bmatrix} = \sum_{i=1}^{3} N_i(\xi)\,\frac{1+\eta}{2}\begin{Bmatrix} r_i \\ z_i \end{Bmatrix}_{top.} + \sum_{i=1}^{3} N_i(\xi)\,\frac{1+\eta}{2}\begin{Bmatrix} r_i \\ z_i \end{Bmatrix}_{bot.} \tag{1}$$

where $N_i(\xi)$ define as a shape function related to node i for element. Which there significant as shown in Eq. (2):

$$N_1 = \xi\,(\xi -1)/2,\; N_2 = 1- \xi^2,\; N_3 = \xi(\xi +1)/2 \tag{2}$$

So, it can be notified that the suitable write the Eq. (1) in the formula detailed as a “vector” linking a lower and an upper point (i.e. the length for vector equal to a thickness of shell) and a mid-surface coordinate, therefore, now we have Eq. (3a and 3b):

$$\begin{Bmatrix} r \\ z \end{Bmatrix} = \sum_{i=1}^{3} N_i(\xi)\,\begin{Bmatrix} r_i \\ z_i \end{Bmatrix}_{mid} + \sum_{i=1}^{3} N_i(\xi)\,\frac{\eta}{2}\,\overrightarrow{V_{3i}} \tag{3a}$$

$$\overrightarrow{V_{3i}} = t_i \begin{Bmatrix} cos\,\varphi_i \\ sin\,\varphi_i \end{Bmatrix} \tag{3b}$$

3. Field of Displacement

For non-symmetric loading, the axial displacements, circumferential and variation of the radial done the volume of the element is separated into meridional and circumferential behaviour. The displacement in circumferential is expected to be harmonic for any order.

The vector of displacement U given by Eq. (4) below represented the global coordinate system [13]:

$$U = \begin{Bmatrix} u \\ v \\ w \end{Bmatrix} =$$

$$\sum_{n=0}^{N} \begin{bmatrix} cos\,n\,\theta & 0 & 0 & sin\,n\,\theta & 0 & 0 \\ 0 & cos\,n\,\theta & 0 & 0 & sin\,n\,\theta & 0 \\ 0 & 0 & sin\,n\,\theta & 0 & 0 & cos\,n\,\theta \end{bmatrix} \begin{Bmatrix} \bar{u}_n \\ \bar{v}_n \\ \bar{w}_n \\ \overline{\overline{u}}_n \\ \overline{\overline{v}}_n \\ \overline{\overline{w}}_n \end{Bmatrix} \tag{4}$$

That a collection range done a whole number for harmonics also n is an order for every harmonic. A double with single striped relations mention, correspondingly, to an antisymmetric with symmetric donations of a components of displacement to a n^{th} harmonic. The functions only for r and z and are included in an element in relations for displacement of the nodal. It is worth noting to explain that when it be said a symmetry in the structural system, it implies an existence for symmetry both in the loading on that structure and also structure itself (involving a conditions of support). For the antisymmetric system a structure (involving conditions of support still symmetric, however, the loading is antisymmetric.

For simplification cases, load components that considered a symmetric are primary measured then far along there are antisymmetric. A displacement of nodal involve of a displacement relative to node *I* add displacement of node *i* formed using rotation for $V_3^i V_3^i$ also there are specified using Eq. (5). Noting that the rotation for normal at a node (*α, β*) give a relative displacement for each node of the element which are represent a nodal circle.

$$\begin{Bmatrix}\bar{u}_n\\ \bar{v}_n\\ \bar{w}_n\end{Bmatrix} = \sum_{i=1}^{3} N_i \begin{Bmatrix}\bar{u}_{ni}\\ \bar{v}_{ni}\\ \bar{w}_{ni}\end{Bmatrix} + \sum_{i=1}^{3} N_i t_i \frac{\eta}{2}\begin{bmatrix}-\sin\varphi_i & 0\\ \cos\varphi_i & 0\\ 0 & 1\end{bmatrix}\begin{Bmatrix}\bar{\alpha}_{ni}\\ \bar{\beta}_{ni}\end{Bmatrix}\begin{Bmatrix}\bar{u}_n\\ \bar{v}_n\\ \bar{w}_n\end{Bmatrix} = \sum_{i=1}^{3} N_i \begin{Bmatrix}\bar{u}_{ni}\\ \bar{v}_{ni}\\ \bar{w}_{ni}\end{Bmatrix} + \sum_{i=1}^{3} N_i t_i \frac{\eta}{2}\begin{bmatrix}-\sin\varphi_i & 0\\ \cos\varphi_i & 0\\ 0 & 1\end{bmatrix}\begin{Bmatrix}\bar{\alpha}_{ni}\\ \bar{\beta}_{ni}\end{Bmatrix} \quad (5)$$

where u_i, v_i, w_i, are displacements of the nodal, η is curvilinear coordinates and α_i, β_i are angle of rotational as presented in Fig. 2.

The contribution to the global displacement as of a specified node *i* for *n* harmonic is:

$$\begin{Bmatrix}\bar{u}_n\\ \bar{v}_n\\ \bar{w}_n\end{Bmatrix}_{3x1} = \sum_{i=1}^{3}\begin{bmatrix} N_i & 0 & 0 & -N_i\eta\frac{t_i}{2}\sin\varphi_i & 0\\ 0 & N_i & 0 & +N_i\eta\frac{t_i}{2}\cos\varphi_i & 0\\ 0 & 0 & N_i & 0 & +N_i\eta\frac{t_i}{2}\end{bmatrix}\begin{Bmatrix}\bar{u}_{ni}\\ \bar{v}_{ni}\\ \bar{w}_{ni}\\ \bar{\alpha}_{ni}\\ \bar{\beta}_{ni}\end{Bmatrix} \quad (6)$$

or in condensed form:

$$\{\bar{U}_n\} = \sum_{i=1}^{3}[N]_i\{\bar{U}_{ni}\}\,\{\bar{U}_n\} = \sum_{i=1}^{3}[N]_i\{\bar{U}_{ni}\} \quad (7)$$

in additional form:

$$\begin{Bmatrix}\bar{u}_n\\ \bar{v}_n\\ \bar{w}_n\end{Bmatrix} = [\,[N]_1 \quad [N]_2 \quad [N]_3]\begin{Bmatrix}\bar{U}_{n1}\\ \bar{U}_{n_2}\\ \bar{U}_{n_3}\end{Bmatrix} \quad (8)$$

An overall countenance for all harmonics is specified by Eq. (9):

$$\begin{Bmatrix}u\\ v\\ w\end{Bmatrix} = \sum_{n=0}^{N}\left[\overline{S}n\right]\; [[N]_1 \quad [N]_2 \quad [N]_3]\begin{Bmatrix}\bar{U}_{n_1}\\ \bar{U}_{n_2}\\ \bar{U}_{n_3}\end{Bmatrix}\begin{Bmatrix}u\\ v\\ w\end{Bmatrix} = \sum_{n=0}^{N}\left[\overline{S}n\right]\; [[N]_1 \quad [N]_2 \quad [N]_3]\begin{Bmatrix}\bar{U}_{n_1}\\ \bar{U}_{n_2}\\ \bar{U}_{n_3}\end{Bmatrix} \quad (9a)$$

where: $\left[\overline{S}n\right]_{3x3} = \begin{bmatrix}\cos n\varphi & 0 & 0\\ 0 & \cos n\varphi & 0\\ 0 & 0 & \sin n\varphi\end{bmatrix}$ (9b) where:

Equation (9a) may wrote as shown:

$$\{U\} = \sum_{n=0}^{N}[\overline{S}_n][N]\{\bar{U}_n\} \tag{9c}$$

where [*N*] was the (3×15) matrix for shape functions also $\{\bar{U}_n\}$ is the (15x1) displacement vector for element.

According to a situation for antisymmetric (a double banded relations state), a matrix $[\overline{S}_n]$ that will be substituted using $[\overline{S}_n]$ matrix. That $[\overline{S}_n]$ be got from $[\overline{S}_n]$ using replacement *cos nθ* by *sin nθ* as well as vice versa.

4. Definitions of Stress and Strain

When a field of displacement has been definite, a strain displacement association be recognized using combination of correct derivative for displacements. A strain component of the axisymmetric shells stated for global coordinate system were presented [15]:

$$\begin{Bmatrix} \varepsilon_{r_n} \\ \varepsilon_{z_n} \\ \varepsilon_{\theta_n} \\ \gamma_{r_n z_n} \\ \gamma_{r_n \theta_n} \\ \gamma_{z_n \theta_n} \end{Bmatrix} = \begin{Bmatrix} \frac{\partial u_n}{\partial r} \\ \frac{\partial v_n}{\partial z} \\ \frac{u_n}{r} + \frac{1}{r}\frac{\partial w_n}{\partial \theta.} \\ \frac{\partial u_n}{\partial z} + \frac{\partial v_n}{\partial r}. \\ \frac{1}{r}\frac{\partial u_n}{\partial \theta} + \frac{\partial w_n}{\partial r} - \frac{w_n}{r} \\ \frac{1}{r}\frac{\partial v_n}{\partial \theta} + \frac{\partial w_n}{\partial z}. \end{Bmatrix} \tag{10}$$

An essential for alter a strain to local coordinate system using a suitable alteration. Now two groups for alterations were essential before an element will been integrated corresponding to a curvilinear coordinates *ξ* with *η* [15]:

First, a global displacement derivatives *u, v* also *w* according to a global *r, z* also *θ* coordinates may specified using depending Jacobian operator shown in Eq. (11):

$$\begin{bmatrix} \frac{\partial u_n}{\partial r} & \frac{\partial v_n}{\partial r} & \frac{\partial w_n}{\partial r} \\ \frac{\partial u_n}{\partial z} & \frac{\partial v_n}{\partial z} & \frac{\partial w_n}{\partial z} \\ \frac{\partial u_n}{\partial \theta} & \frac{\partial v_n}{\partial \theta} & \frac{\partial w_n}{\partial \theta} \end{bmatrix} = J^{-1} \begin{bmatrix} \frac{\partial u_n}{\partial \xi} & \frac{\partial v_n}{\partial \xi} & \frac{\partial w_n}{\partial \xi} \\ \frac{\partial u_n}{\partial \eta} & \frac{\partial v_n}{\partial \eta} & \frac{\partial w_n}{\partial \eta} \\ \frac{\partial u_n}{\partial \theta} & \frac{\partial v_n}{\partial \theta} & \frac{\partial w_n}{\partial \theta} \end{bmatrix} \tag{11}$$

where *J* is a Jacobian operator concerning a derivative of natural coordinate to a derivative of local coordinate. That may be considered from a definition for coordinate as presented in Eq. (3) as mentioned below:

$$J = \begin{bmatrix} \frac{\partial r}{\partial \xi} & \frac{\partial z}{\partial \xi} & 0 \\ \frac{\partial r}{\partial \eta} & \frac{\partial z}{\partial \eta} & 0 \\ 0 & 0 & 1 \end{bmatrix} \tag{12}$$

Second, a displacements global derivative (*u*, *v*, *w*) is now altered for a local derivative for orthogonal displacements depending on alteration matrix [*T*] that would be specified later. An illustration for global coordinate transformation to a local coordinate can be presented below in Eq. (13):

$$\begin{Bmatrix} \acute{r} \\ \acute{z} \\ \theta \end{Bmatrix} = \begin{bmatrix} c & s & 0. \\ -s & c & 0. \\ 0. & 0. & 1. \end{bmatrix} \begin{Bmatrix} r \\ z \\ \theta \end{Bmatrix} \tag{13}$$

At that point a strain stated for local coordinates *(r', z' and θ)* according to the global coordinates *(r, z and θ)* shown below:

$$\{\acute{\varepsilon}\} = [T]\{\varepsilon\}. \tag{14}$$

or by matrix formula:

$$\begin{Bmatrix} \varepsilon_{\acute{z}_n} \\ \varepsilon_{\theta_n} \\ \varepsilon_{\acute{z}_n\theta_n} \\ \gamma_{\acute{r}_n\acute{z}_n} \\ \gamma_{\acute{r}_n\theta_n} \end{Bmatrix} = \begin{bmatrix} s^2 & -sc & 0 & -sc & c^2 & 0 & 0 & 0 & 0 & 0 & 0 \\ 0 & 0 & 0 & 0 & 0 & 0 & 0 & 0 & \frac{1}{r} & \frac{1}{r} & 0 \\ 0 & 0 & \frac{s}{r} & 0 & 0 & \frac{c}{r} & \frac{c}{r} & c & 0 & 0 & -\frac{s}{r} \\ -2cs & c^2-s^2 & 0 & c^2-s^2 & 2cs & 0 & 0 & 0 & 0 & 0 & 0 \\ 0 & 0 & \frac{c}{r} & 0 & 0 & -\frac{s}{r} & -\frac{s}{r} & -s & 0 & 0 & -\frac{c}{r} \end{bmatrix} \begin{Bmatrix} \frac{\partial u_n}{\partial r} \\ \frac{\partial u_n}{\partial z} \\ \frac{\partial u_n}{\partial \theta} \\ \frac{\partial v_n}{\partial r} \\ \frac{\partial v_n}{\partial z} \\ \frac{\partial v_n}{\partial \theta} \\ \frac{\partial w_n}{\partial r} \\ \frac{\partial w_n}{\partial z} \\ \frac{\partial w_n}{\partial \theta} \\ u_n \\ w_n \end{Bmatrix} \tag{15}$$

$$\{\varepsilon_n'\}_{5x1.} = [G]_{5x11.}[A]_{11x11.} \begin{Bmatrix} \frac{\partial u_n}{\partial \xi} \\ \frac{\partial u_n}{\partial \eta} \\ \frac{\partial u_n}{\partial \theta} \\ \frac{\partial v_n}{\partial \xi} \\ \frac{\partial v_n}{\partial \eta} \\ \frac{\partial v_n}{\partial \theta} \\ \frac{\partial w_n}{\partial \xi} \\ \frac{\partial w_n}{\partial \eta} \\ \frac{\partial w_n}{\partial \theta} \\ u_n \\ w_n \end{Bmatrix}_{11x1.} \tag{16}$$

That which:

$$[A] = \begin{bmatrix} [A_\circ]_{9x9} & \\ & [I]_{2x2} \end{bmatrix} \quad , \qquad A_\circ = \begin{bmatrix} [J]^{-1} & & 0 \\ & [J]^{-1} & \\ 0 & & [J]^{-1} \end{bmatrix}$$

and

$$[G]=\begin{bmatrix} s^2 & -sc & 0 & -sc & c^2 & 0 & 0 & 0 & 0 & 0 & 0 \\ 0 & 0 & 0 & 0 & 0 & 0 & 0 & 0 & \frac{1}{r} & \frac{1}{r} & 0 \\ 0 & 0 & \frac{s}{r} & 0 & 0 & \frac{c}{r} & \frac{c}{r} & c & 0 & 0 & -\frac{s}{r} \\ -2cs & c^2-s^2 & 0 & c^2-s^2 & 2cs & 0 & 0 & 0 & 0 & 0 & 0 \\ 0 & 0 & \frac{c}{r} & 0 & 0 & -\frac{s}{r} & -\frac{s}{r} & -s & 0 & 0 & -\frac{c}{r} \end{bmatrix}$$

At that point the vector of strain presented as:

$$\{\varepsilon'\} = \sum_{i=1}^{3}[G_i]\,.\,[A_i].\sum_{n=0}^{N}[\bar{C}_n]\,.\,[\bar{\beta}_{ni}].\{\bar{U}_{ni}\} \tag{17}$$

For the i^{th} node in n^{th} harmonic, once may be determined a strain matrix $\overline{[\bar{\beta}_{ni}]}$ as shown below:

$$[\bar{\beta}_{ni}]_{11x5} = \begin{bmatrix} \frac{\partial N_i}{\partial \xi} & 0 & 0 & -\frac{\partial N_i}{\partial \xi}\eta\frac{t_i}{2}S_i & 0 \\ 0 & 0 & 0 & -N_i\frac{t_i}{2}S_i & 0 \\ -nN_i & 0 & 0 & nN_i\eta\frac{t_i}{2}S_i & 0 \\ 0 & \frac{\partial N_i}{\partial \xi} & 0 & \frac{\partial N_i}{\partial \xi}\eta\frac{t_i}{2}C_i & 0 \\ 0 & 0 & 0 & N_i\frac{t_i}{2}C_i & 0 \\ 0 & -nN_i & 0 & -nN_i\eta\frac{t_i}{2}C_i & 0 \\ 0 & 0 & \frac{\partial N_i}{\partial \xi} & 0 & \frac{\partial N_i}{\partial \xi}\eta\frac{t_i}{2} \\ 0 & 0 & 0 & 0 & N_i\frac{t_i}{2} \\ 0 & 0 & nN_i & 0 & nN_i\eta\frac{t_i}{2} \\ N_i & 0 & 0 & -N_i\eta\frac{t_i}{2}S_i & 0 \\ 0 & 0 & N_i & 0 & N_i\eta\frac{t_i}{2} \end{bmatrix} \tag{18}$$

where $C_i = cos\,\phi_i$ and $S_i = sin\,\phi_i$

Also, a concluding strain displacement relationship there:

$$\{\varepsilon'\} = \sum_{n=0}^{N}[\bar{B}_n]\,.\,\{\bar{U}_n\} \tag{19}$$

where: $[\bar{B}_n] = [G][A][\bar{\beta}_{ni}]$

A stress related to a preceding strain can be defined in the local coordinate as shown in Eq. (20):

$$\{\sigma'\} = [D']\sum_{n=0}^{N}[\bar{\beta}_{ni}]\{\bar{U}_n\} \tag{20}$$

which the matrix $[D']$ is a (5x5) consider a matrix of elasticity involving a fitting property of material.

5. Stiffness Matrix

The element stiffness matrix of a symmetric harmonic relationship drive used formulated due to depending on a strain energy principle. An energy of strain of a scheme is [16]:

$$E = \frac{1}{2}\int_{A.}^{2}\int_{0}^{\pi}\varepsilon^T\,\sigma\,r\,\theta\,dA. \tag{21}$$

Replacing Eq. (19) with Eq. (20) through Eq. (21), so once determination be got:

$$E = \frac{1}{2}\int_{0}^{2\pi}\int_{A}\sum_{n=0}^{N}\sum_{m=0}^{N}\{\bar{U}_n\}^T[\bar{B}_n]^T[D'][\bar{B}_m]\{\bar{U}_m\}rdAd\theta. \tag{22}$$

Next preparing the manipulation of matrix, it significant for contemplate an integral over θ that involve (consider beyond a diagonal sub matrices) a terms *sinmθ sinnθ* and *cosmθ cosnθ*, that *m* with *n* are different integers. By giving with account a property for orthogonality, those relations become extinct for a bound from 0 till 2π. Conversely a diagonal sub matrix involves relations similar $sin^2 n\theta$ or $cos^2 n\theta$ which those relations can product a public factor π till 2π after making an integration. At that time, ta strain energy can be expressed by Eq. (23) as shown below:

$$E = \frac{1}{2}\lambda\pi \sum_{n=0}^{N}\{\bar{U}_n\} \int_A [\bar{B}_n]^T[D'][\bar{B}_n]rdA\{\bar{U}_n\}. \tag{23}$$

where:-

$\lambda = 2$ for $n = 0$
$= 1$ for $n = 1, 2, 3, \dots \dots, N$.

Now, element stiffness matrix can be written:

$$[\bar{K}_n]_{15x15.} = \frac{\partial 2E}{\partial \bar{U}\partial \bar{U}} = \lambda\pi \int_A [\bar{B}_n]^T[D'][\bar{B}_n]rdA. \tag{24}$$

also, due to depending on a relationship $dA = dr\,dz = |J|\,d\xi\,d\eta.$, so, we obtain the Eq. (25),

$$[\bar{K}_n]_{15x15.} = \lambda\pi \int_{-1}^{+1}\int_{-1}^{+1}[\bar{B}_n]^T[D'][\bar{B}_n]r|J|d\xi d\eta. \tag{25}$$

where $[\bar{K}_n]$ consider an element stiffness matrix of symmetric n^{th} harmonic term. A stiffness matrix for structure next gets together for stiffness matrix of elements be expressed distinctly of each harmonic also kept through the auxiliary storage file of consequent stage aimed to solution.

6. Formulation of Mass Matrix

In this study a dependable mass method is assumed and a mass matrix of element for a symmetric "*n*" harmonic term be produced depending on a principle of kinetic energy as shown in equations below:

First, a kinetic energy *T* of the scheme be [17]:

$$T = \frac{1}{2}\int_0^{2\pi}\int_A \rho\,\{\dot{U}\}^T\{\dot{U}\}\,rdAd\theta. \tag{26}$$

where parameters be defined,

ρ : is a density of mass

$\{\dot{U}\}$: a vector of velocity. Also, a dot signifies difference due to time.

The vector of velocity may be written as shown in Eq. (27) below:

$$\{\dot{\bar{U}}\} = \sum_{n=0}^{N}[\bar{C}_n]\,[N]\{\dot{\bar{U}}_n\}. \tag{27}$$

where [*N*] is the (3x15) shape functions matrix as well as the matrix $[\bar{C}_n]$ be (15x3) matrix of damping.

Relieving Eq. (27) through Eq. (26), so,

$$T = \frac{1}{2}\int_0^{2\pi}\int_A \rho\sum_{n=0}^{N}\sum_{m=0}^{N}\{\dot{\bar{U}}_n\}^T[N]^T[\bar{C}_n]^T[\bar{C}_n][N]\{\dot{\bar{U}}_m\}\,dAd\theta. \tag{28}$$

Next execution manipulation of matrix also applying a conditions of orthogonality Eq. (28) can expressed by Eq. (29):

$$T = \frac{1}{2}\lambda\pi\rho \sum_{n=0}^{N}\left\{\bar{U}_n\right\}^T \int_A [N]^T[N]rdA \left\{\bar{U}_n\right\}. \tag{29}$$

where: $\lambda = 2$ for $n = 0$

$= 1$ for $n = 1, 2, 3, ..., N$.

A mass matrix of element may write as:

$$[M_n]_{15x15} = \frac{\partial 2T}{\partial\bar{U}\partial\bar{U}} = \lambda\pi\rho \int_A [N]^T[N]\, rdA. \tag{30}$$

or:

$$[\bar{M}_n] = \lambda\pi\rho \int_{-1}^{+1}\int_{-1}^{+1}[N]^T[N]r|J|d\xi d\eta. \tag{31}$$

7. Formulation of Load Vector

For non-axisymmetric exterior load be fragmented down by axial, radial also circumferential main components (P_z, P_r, P_T respectively) by a typical measure for Fourier series representation. Subsequent estimates are created as per in Eq. (32):

$$P_r = \sum_{n=0.}^{N}\bar{P}_{r_n} cos\, n\theta. + \sum_{n=1}^{N}\bar{\bar{P}}_{r_n} sin\, n\theta.$$

$$P_z = \sum_{n=0.}^{N}\bar{P}_{r_n} cos\, n\theta. + \sum_{n=1}^{N}\bar{\bar{P}}_{r_n} sin\, n\theta. \tag{32}$$

$$P_{T_\theta} = \sum_{n=1.}^{N}\bar{P}_{T_n} sin\, n\theta. + \sum_{n=0}^{N}\bar{\bar{P}}_{T_n} cos\, n\theta.$$

where:

$\bar{P}_{r_n}, \bar{P}_{z_n}, \bar{P}_{T_n}\ as\ well\ as\ \bar{\bar{P}}_{r_n}, \bar{\bar{P}}_{z_n}, \bar{\bar{P}}_{T_n}$ are, respectively, a symmetric load also antisymmetric load breadths for a n^{th} harmonic term of radial, axial also tangential directions respectively. Then, may it had obtained by an integration progress with a benefit for trigonometric functions orthogonality in an interval *($0 \leq \theta \leq 2\pi$)*.

Subsequently, loading forms for example the pressures, gravity action allotted of surface for element, should it minimized for comparable nodal forces earlier solution may progress [18]. These adaptations of loads distributed by comparable nodal loads may be doing by depending on the virtual displacement principle. Therefore, the forces for nodal of a n^{th} harmonic part of node *i* (for symmetric situation) can presented in Eq. (33) shown below:

$$\begin{Bmatrix} P_{r_{ni}} \\ P_{z_{ni}} \\ P_{T_{ni}} \\ M_{\alpha_{ni}} \\ M_{\beta_{ni.}} \end{Bmatrix}_{5x1.} = \int_A \int_0^{2\pi}[N_i]_{5x3}^T[\bar{C}_n]_{3x3.}\begin{Bmatrix} \bar{P}_{r_n}\cos n\theta \\ \bar{P}_{z_n}\cos n\theta \\ \bar{P}_{T_n}\sin n\theta \end{Bmatrix} rd\theta dA. \tag{33}$$

Using an orthogonality for functions trigonometric (an integration with respect to θ for a range $0 \rightarrow 2\pi$), Eq. (33) develops:

$$\begin{Bmatrix} P_{r_{ni}} \\ P_{z_{ni}} \\ P_{T_{ni}} \\ M_{\alpha_{ni}} \\ M_{\beta_{ni.}} \end{Bmatrix} = \int_A \pi r [N_i]^T \begin{Bmatrix} \bar{P}_{r_n} \\ \bar{P}_{z_n} \\ \bar{P}_{T_{n.}} \end{Bmatrix} dA \quad \text{for} \quad n=1, 2, \ldots\ldots, N.$$

$$= 2 \int_A \pi r [N_i]^T \begin{Bmatrix} \bar{P}_{r_o} \\ \bar{P}_{z_o} \\ 0 \end{Bmatrix} dA. \ \text{for } n = 0 \tag{34}$$

8. Equilibrium Equation of Dynamic

The motion equations for the revolution shell under preservation loading has been derived as of principles of Hamilton variational as per Eq. (35) shown below:

$$M\ddot{U} + C\dot{U} + KU = p(t). \tag{35}$$

which a stiffness *K* matrix, damping *C* and mass *M* are formed through a direct assemblage process for related element matrices. And $\ddot{U}$, $\dot{U}$ also U are an acceleration, velocity as well as displacement vectors respectively. Then it may notify since a preceding section, all a matrix of structure may it stated in terms of the sensible number for harmonic terms in a circumferential direction. At that moment the resulting separated equations for motion of the typical harmonic (*n*) at every station of time (Δt) will it be shown in Eq. (36) below:

$$\sum_{n=0.}^{N} \left(M_n \ddot{U}_n + C_n \dot{U}_n + k_n U_n = P_n(t) \right) \tag{36}$$

Also an equation for undamped motion is presented in Eq. (37):

$$\sum_{n=0}^{N} \left(M_n \ddot{U}_n + k_n U_n = P_n(t) \right). \tag{37}$$

From Eq. (37), (*N*+1) distinct separated problems were solved of every time step to find a displacement of nodal U_n consistent of every harmonic. First of all, harmonic terms may be processed, the last displacements at every node for every angle (θ) may be find by the combination of every harmonic. On one occasion the collected matrices of the total structure are passed out, the unknown parameters of displacement may eagerly be initiate by solving the found equilibrium equation. Fundamentally for the solution of simultaneous Eq. (15), there are two different methods: Mode superposition and direct solution techniques methods. Once when associated to a solution of model superposition, a direct integration method be attractive in an eigen value problem be avoided. As well as, definitely, in utmost cases, a direct integration method is a faster. In this work, a method of direct integration will be being depending on it is accuracy, efficiency also wide using. Then doing step by step solution by depending on method of Newmark integration have been originated to being actual in a solution for both shell and solid finite element systems. It will be implied method and unconditionally stables of all steps of time.

9. Verification and Applications

For applicability demonstrate of the potential and formulation of the developed program, some examples were measured and associated with obtainable results in a literature. Satisfactory and actual results are gotten.

9.1. Pinched cylindrical shell

The cylindrical shell strained using two completely opposite pointed forces *P* at a cylinder centre be analysed of it is static reply state. Cylinder ends are fixed. A boundary condition, geometry, finite element mesh as well as material properties are presented in Fig. 3.

Varies thicknesses of a cylinder were depended for justification of a varies radius for thickness ratio (*R/h*). A load be approximately by Fourier series development as shown in Eqs. (38) and (39):

$$P_r = \sum_{n=0}^{N} P_m \cos n\theta. \quad (38)$$

A Fourier load breadths of a point load are:

$$P_{ro} = \frac{P}{\pi \bar{r}} \quad \text{for } n = 0.$$

$$P_{rn} = \frac{2P}{\pi \bar{r}} \quad \text{for even harmonic terms} \quad (39)$$

$$= 0. \quad \text{for odd harmonic terms}$$

Note: $\bar{r}$: distance from to a point load and a centre.

It can be notified from Table 1, a catalogue a maximum deflection of normalized non dimensional at a point load. Then radius to thickness percentages travelled were *R/h* = 100, 300 also 500. A value of maximum deflection (w_{fem}) may be computed by a current method is regularised to a solution specified in the references [17] that shown in Eq. (39):

$$\bar{W} = \frac{w_{fem}}{w_{ref.}}. \quad (39)$$

where

$\bar{W}$: normalized deflection,

$w_{fem.}$: current finite element results also

$w_{ref..}$: reference [19] solution.

Reference [19] solution may be presented as: $w_{ref.} = C\frac{P}{Et}$

where C is a proportional constant related the values of central deflection with the applied central load. The constant value *C* for every (*R/h*) ratio be shown through Table 1 composed with a number of Fourier harmonic depend for every case.

Table 1. Normalized maximum deflection at the point load for cylindrical shell with fixed ends.

R/h	***C***	**No. Fourier harmonic**	$\bar{W}$
100	136.8	6	1.0706
300	516.2	8	0.9020
500	960.9	11	1.0310

Table 1 presents a satisfactory agreement of found deflection results also presents junction tendencies of the deflection with those of reference [19] and shows conjunction tendencies of a displacement through a number for Fourier harmonic increases by increasing the (*R/h*) ratio. More accurate results could be gain with increased number of Fourier harmonic as the results approach to its real values when more terms of Fourier series are considered especially when R/h values are increased as could be seen in Table 1. Figure 4 illustrations non dimensional normal (radial) deflection at a point load as opposed to a circumferential direction of a shell for different (*R/h*) ratios related. A maximum deflection happens when theta angle equal be zero (that be characterise an applied point load) as may be notify as of the figure.

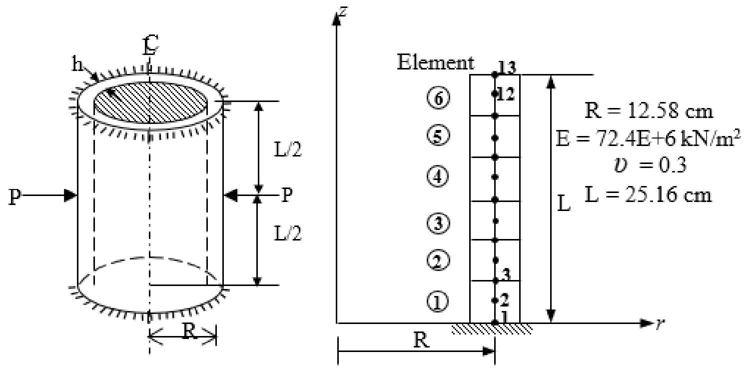

Fig. 3. Axisymmetric cylindrical shell with symmetrical point load.

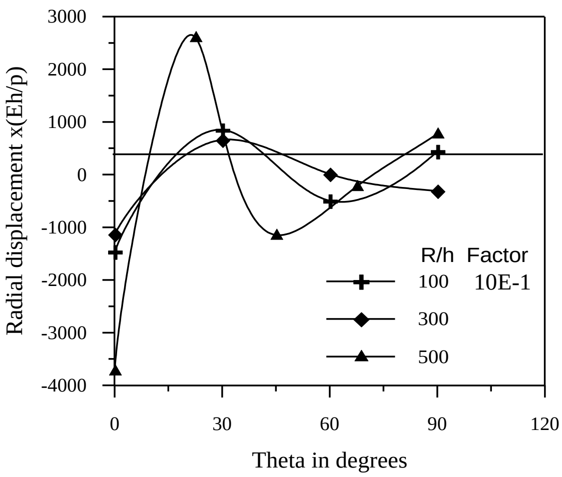

Fig. 4. Normal displacement at point load versus circumferential theta direction for example of (Fig. 3).

9.2. Dynamic response for cylindrical shell

The cylindrical shell laid for a uniformly inner spread sine wave impulsive loading through a highest intensity with (100 kPa) be measured and given by Fig. 5 collected with a material property, mesh of finite element also geometry.

A purpose for that case is for comparison it is response with a solution of standard finite element for computer program of dynamic analysis transient using an element with nine-node. The compartment of two results with veneration to number for unknowns also computer time consumption as shown in Table 2. A total number of degrees for freedom and a needed computer time minimized by 80% comparison with standard finite element as mentioned Table 2.

Table 2. A comparison of unknowns and computer time consumption for the example shown in Fig. 4.

Type of approach	Present work	Standard finite element
Number of elements	3	6
Number of unknowns	35	175
Computer time consumption (sec)	20	115

Figure 6 showed the normal displacement of the tip point. It can be notified that a normal displacement point arrives it is a maximum value approximately (0.75 sec.). It can be seen from the Fig. 7 the conjunction of a circumferential stress σ_θ results on a tip point such generalised values beginning from a near Gauss point (element 3, G.P. No.3) by a typical finite element solution.

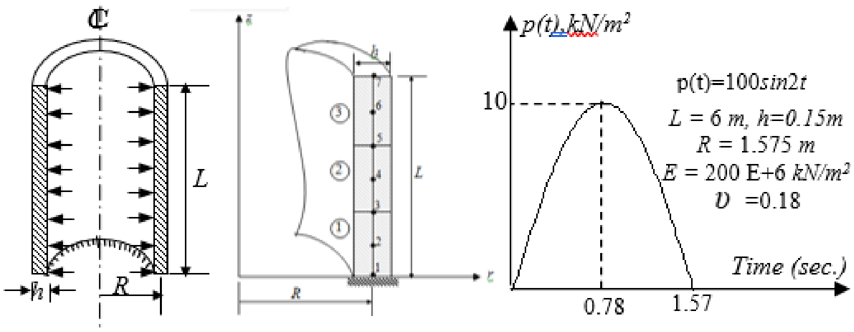

Fig. 5. Axisymmetric cylinder under sine impulsive load.

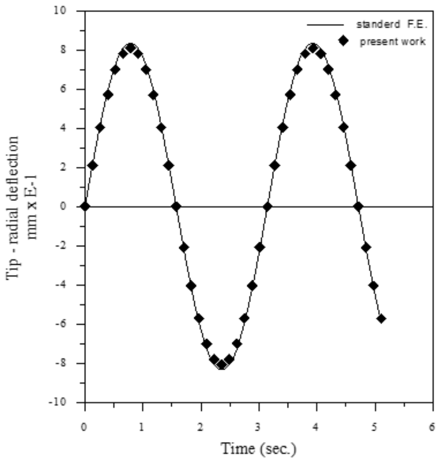

Fig. 6. Tip normal deflection-time history for cylindrical shell under sinusoidal load.

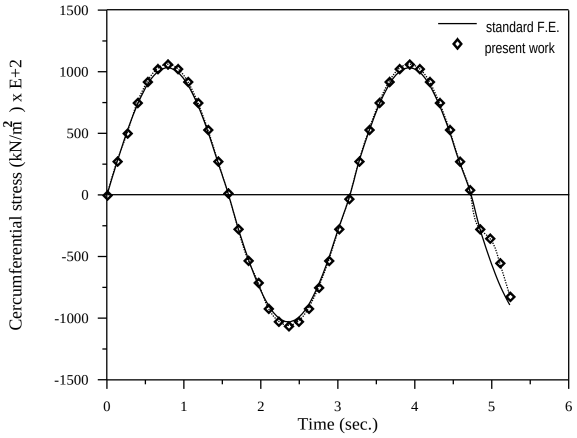

Fig. 7. Circumferential stress-time history of the tip point for the problem of Fig. 5.

9.3. A shallow thin spherical cap

The dynamic analysis for the thin spherical shallow cap be approved obtainable due to applying Heaviside step intensity pulse loading with (4.41 MPa). A cap radius be (R=56.6 cm), thickness (h=10 mm), also semi angle with (ϕ=26.67°). Completely a related collected data within finite element mesh were showed by Fig. 8. The step for time (5E-6 sec.) be depending through mentioned example. A time difference for an apex deflection for the cap can be seen in Fig. 9. The mentioned example be compared fit by the reference [20] result in that the analysis be approved out depending on ten eight-node elements with a same step time. A static effect of an apex is as well as showed in Fig. 9. The current study apex deflection time history be correspondingly associated to a three-dimensional result [21, 22] which twenty-seven elements were depended for romanticize a quarter of a cap. It can be seen that very good match is found as presented in Fig. 9.

The difference of a normal stress (σ_θ) due to time on a Gauss point closer to an apex (element 6, G.P.3) be presented through a Fig. 10. A time for minimum and maximum stress also a length of period was presented in Fig. 10. Correspondingly, the difference of a vertical deflection for a point near a support (node 3) is showed by Fig. 11.

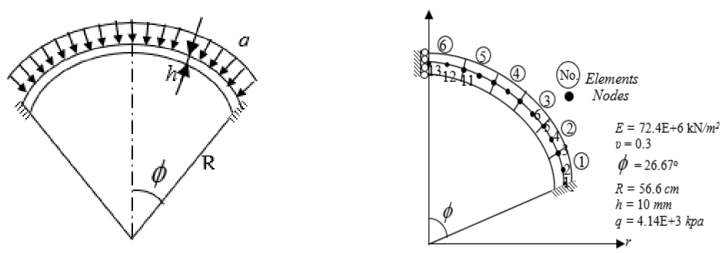

(a) Section in the cap. (b) Finite element
Fig. 8. Shallow thin spherical cap (mesh and geometry).

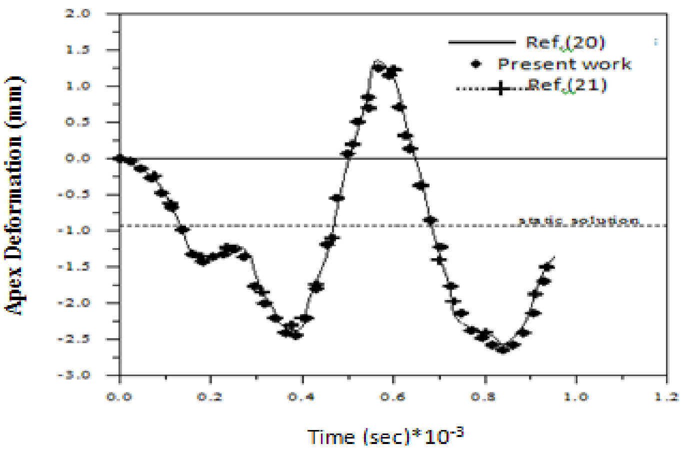

Fig. 9. Apex deflection-time history for shallow thin spherical cap under Heaviside loading.

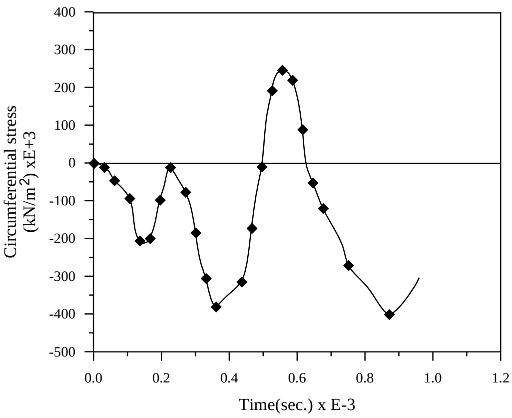

Fig. 10. Circumferential stress-time history at the point nearest to the apex for shallow thin spherical cap.

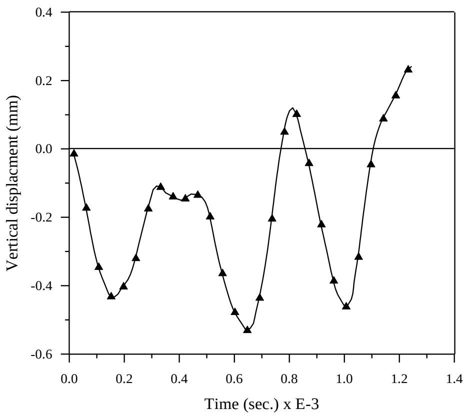

Fig. 11. Variation of vertical deflection-time history node 3 for shallow thin spherical cap.

10. Conclusions and Recommendations

Regarding to obtained results from this work, a main conclusion be brief in listed points shown below:

- The adapted shell analysis program depends on a semi analytical method has been create for give a suitable solution specially related to dynamic cases. As well as, by comparison the obtained results with the results from the other references, all appear errors lie inside the normal accuracy engineering. Usually, the error percentage is less than of 10% of all worked cases and the percentage can depended satisfactory related to greatest applied problems.
- An anticipated method was institute to become an additional effective and inexpensive from a standpoint for data handling also preparing, computer time and calculation efficiency as well as reminiscence requirements. Correspondingly the limited elements numbers were satisfactory to signify a

whole structure by exact results founded also that lead to decreasing an analysis for cost.

- Suggested proposal method may be stretched to consist of both geometric nonlinearities and material. But that would be result in the big increasing for computer time, then a matrix of stiffness will be being moulded several times through a step-by-step solution procedure [23].
- In general, the required computer time also a total number for freedom degrees a present work is reduced with 70- 80% compared with standard finite element as it be mentioned in Table 2.
- It is recommended to solve more complex problems such as tanks filled with liquid or water to deal with the hydrostatic pressure.
- It is recommended to re-analyse the same problems under the effect of earthquakes for their importance nowadays.

Nomenclatures

dA	Element Infinitesimal area.
E	Energy of strain
$[J]$	Jacobian matrix
$[\overline{K}_n]$	Stiffness matrix of element
K, C, and M	Stiffness matrices damping also mass respectively
m and n	Different integers
$[M_n]$	Mass matrix element
$[N]$	A (3x15) shape functions matrix
$N_i(\xi)$	Shape function related with node i for an element
P_r, P_z, P_T	load components in radial, axial also circumferential
$\overline{P}_{r_n}, \overline{P}_{z_n}, \overline{P}_{T_n}$	Symmetric load bounties for a n^{th} harmonic part for radial, axial also circumferential directions respectively.
$\overline{\overline{P}}_{r_n}, \overline{\overline{P}}_{z_n}, \overline{\overline{P}}_{T_n}$	Anti-symmetric load bounties for a n^{th} harmonic part for radial, axial also circumferential directions respectively.
r, z, θ	Global cylindrical coordinate system
r', z', θ	Local coordinate system
T	Kinetic energy
$[T]$	Matrix for a strain transformation
u, v, w	Global displacement system
u_i, v_i, w_i	Translation freedom degrees
U	Displacement vector
$\{\dot{U}\}$	The vector of velocity
$\{\bar{U}_n\}$	A (15x1) a displacement vector for element.
$U, \dot{U}, \ddot{U}$	Displacement, velocity also acceleration vectors respectively.
$\bar{U}, \dot{\bar{U}}, \ddot{\bar{U}}$	Element displacement, velocity also acceleration vector for symmetric definite harmonic part.
$\overline{W}$	Normalized deflection,

Greek Symbols

α_i, β_i	Freedom Rotational degrees.
θ	Angle for a circumferential direction
ϕ	Angle for a meridian direction

ξ *and* η	Coordinates of curvilinear
$\bar{\beta}$	Matrix of strain
$\{\varepsilon'\}$	Strain displacement
ρ	Mass density
Δt	Interval of time

References

1. Bairagi, N.; and Mohammed Ismail, G. (1994). Behaviour of cylindrical shells used as bridge decks. *Bulletin of the International Association for Shell and Spatial Structures*, 35(1), 47-53.
2. Albertin, U.; and Wunderlich, W. (2000). Buckling design of imperfect spherical shells. *Computational Methods for Shell and Spatial Structures, IASS–IACM 2000M.* Athens, Greece, 1-20.
3. Danaeinia, A.; and Korsavi, S.S. (2017). Techniques to carry weight loads and resist against bending in conical shells, studying case studies of Kashan. *International Journal of Architectural Engineering and Urban Plan*, 27(1), 9-18.
4. Rotter, J.M. (2017). Shell buckling transformed: Mechanics, design processes and their inter-relation. *Stahlbau*, 86(4), 315-324.
5. Cook, R.D.; Malkus, D.S.; and Plesha, M.E. (2001). *Concept and applications of finite element analysis* (4th ed.). New York: John Wiley and Sons, Inc.
6. Lindberg, H.E.; and Florence, A.L. (2012). *Dynamic pulse buckling: theory and experiment* (Vol. 12). Springer Science and Business Media.
7. Noret, E.; Prod'Homme, G.; Yalamas, T.; Reimeringer M.; Hanus, J.L.; and Duong, D.H. (2012). Safety of atmospheric storage tanks during accidental explosions. *European Journal of Environmental and Civil Engineering*, 16(9), 998-1022.
8. Duong, D.H.; Hanus, J.L.; Bouazaoui, L.; Pennetier, O.; Moriceau, J.; Prod'homme, G.; & Reimeringer, M. (2012). Response of a tank under blast loading-part I: experimental characterisation of blast loading arising from a gas explosion. *European Journal of Environmental and Civil Engineering*, 16(9), 1023-1041.
9. Duong, D.H.; Hanus, J.L.; Bouazaoui, L.; Regal, X.; Prod'Homme, G.; Noret, E.; Yalamas, T.; Reimeringer, M.; Bailly, P.; and Pennetier, O. (2012). Response of a tank under blast loading–Part II: Experimental structural response and simplified analytical approach. *European Journal of Environmental and Civil Engineering*, 16(9), 1042-1057.
10. Ameijeiras, M.P.; and Godoy, L.A. (2016). Simplified analytical approach to evaluate the nonlinear dynamics of elastic cylindrical shells under lateral blast loads. *Latin American Journal of Solids and Structures*, 13(7), 1281-1298.
11. Hajlaoui, A.; Triki, E.; Frikha, A.; Wali, M.; and Dammak, F. (2017). Nonlinear dynamics analysis of FGM shell structures with a higher order shear strain enhanced solid-shell element. *Latin American Journal of Solids and Structures*, 14(1), 72-91.
12. Spilker, R.L.; and Daugirda, D.M. (1981). Analysis of axisymmetric structures under arbitrary loading using the hybrid-stress model. *International Journal for Numerical Methods in Engineering*, 17(6), 801-828.

13. Zienkiewicz, O.C. (1977). *Finite elemen method*. McGraw Hill.
14. Bathe, K.J. (1996). *Finite element procedures*. New Jersey: Prentice Hall.
15. Zienkiewicz, O.C.; Taylor, R.L.; Taylor, R.L.; and Taylor, R.L. (2000). *The finite element method: solid mechanics* (Vol. 2). Butterworth: Heinemann.
16. Chandrupatla, T.R.; Belegundu, A.D.; Ramesh, T.; and Ray, C. (2002). *Introduction to finite elements in engineering* (Vol. 2). Upper Saddle River, NJ: Prentice Hall.
17. Clough, R.W.; and Penzien, J. (1975). *Dynamics of structures*. New York: McGraw-Hill Book Co. Inc.
18. Smith, I.M.; Griffiths, D.V.; and Margetts, L. (2013). *Programming the finite element method*. John Wiley and Sons.
19. Yeom, C.H.; Scardera, M.P.; & Lee, S.W. (1988). Shell analysis with a combination of eight node and nine node finite elements. *Computers and Structures*, 28(2), 155-163.
20. Bathe, K.J.; and Ozdemir, H. (1976). Elastic-plastic large deformation static and dynamic analysis. *Computers and Structures*, 6(2), 81-92.
21. Abdul, A.J. (1989). *Large deformation dynamic analysis of three-dimensional solids by the finite element method*. M.Sc. Thesis. University of Baghdad, Baghdad, Iraq.
22. Hussain, N.L.; Mohammed, S.A.; and Mansor, A.A. (2020). Finite element analysis of large-scale reinforced concrete shell of domes. *Journal of Engineering Science and Technology (JESTEC)*, 15(4), 782-791.
23. Ahmed, A.M.; Wisam, D.S.; and Ali, L.A. (2019). Finite element analysis of reinforced concrete deep beams strengthened in shear with CFRP. *ARPN Journal of Engineering and Applied Sciences*, 14(2), 381-391.